

# Phosphorescent organic light-emitting device with an ambipolar oxadiazole host

Jiun-Haw Lee<sup>a)</sup> and Hsin-Hung Tsai

Graduate Institute of Electro-Optical Engineering, National Taiwan University, No. 1 Sec. 4, Roosevelt Rd., Taipei, Taiwan, Republic of China and Department of Electronical Engineering, National Taiwan University, No. 1, Sec. 4, Roosevelt Rd., Taipei, 10617 Taiwan, Republic of China

Man-Kit Leung, Chih-Chiang Yang, and Chun-Chieh Chao

Department of Chemistry, National Taiwan University, No. 1, Sec. 4, Roosevelt Rd., Taipei, Taiwan, Republic of China and Institute of Polymer Science and Engineering, National Taiwan University, No. 1, Sec. 4, Roosevelt Road, Taipei, 10617 Taiwan, Republic of China

(Received 17 January 2007; accepted 17 May 2007; published online 11 June 2007)

In this letter, the authors demonstrated a phosphorescent organic light-emitting device (OLED) with a lower driving voltage and a longer operation lifetime based on 2,2'-bis[5-phenyl-2-(1,3,4)oxadazolyl]biphenyl, an oxadiazole (OXD) derivative, as the host of the emitting layer doped with a common green-emitting phosphorescent dopant, *fac*-tris(2-phenylpyridine) iridium [Ir(ppy)<sub>3</sub>]. Rather than an electron transporting materials, the OXD exhibits an ambipolar transport characteristic with suitable Ir(ppy)<sub>3</sub> concentrations due to its low highest occupied molecular orbital value (5.9 eV) and the hole-transporting characteristics of Ir(ppy)<sub>3</sub>. It results in a 2.4 V voltage reduction and a 2.6 times lifetime elongation of the OXD-based device, as compared to the conventional phosphorescent OLED. © 2007 American Institute of Physics. [DOI: 10.1063/1.2747663]

Organic light-emitting devices (OLEDs) have attracted much attention owing to their advantages of low-power consumption, high brightness, high contrast, and low cost.<sup>1,2</sup> With the incorporation of the heavy metal complexes, nearly 100% internal quantum efficiency can be obtained with efficient phosphorescence.<sup>3</sup> *fac*-tris(2-phenylpyridine) iridium [Ir(ppy)<sub>3</sub>] is a successful phosphorescent emitters which is typically doped in the carbazole-based host, such as 4,4'-*N,N'*-dicarbazole-biphenyl (CBP).<sup>4,5</sup> However, the highest occupied molecular orbital (HOMO) value of CBP is about 6.3 eV which will result in a larger barrier for hole injection from the hole transport layer (HTL) to the emitting layer (EML), and hence a high driving voltage. Besides, carbazole-based host materials typically exhibit low glass transition temperature ( $T_g$ ) which leads to device instability.<sup>6</sup>

In this letter, we proposed a carbazole-free phosphorescent device by using a new oxadiazole (OXD) derivative, 2,2'-bis[5-phenyl-2-(1,3,4)oxadazolyl]biphenyl, as the host material.<sup>7</sup> This EML, consisting of the Ir(ppy)<sub>3</sub> doped in OXD matrix, showed ambipolar carrier transport characteristics which is due to (1) the smaller HOMO value (5.9 eV) of our OXD which results in the hole tunneling from HTL in EML and (2) the hole-transport characteristics of the Ir(ppy)<sub>3</sub> dopant.<sup>8</sup> Besides, as compared to the conventional CBP, this material shows a high glass transition temperature (over 200 °C) that prolongs the operation lifetime.

Our fabrication and measurement details are shown in Ref. 9. To evaluate the electrical and optical characteristics of the OXD host, we designed the OLED structures which are shown in Table I. 40 nm *N,N'*-diphenyl-*N,N'*-bis(1-naphthyl)-1,1'-biphenyl-4,4'-diamine (NPB) was used as a HTL. OXD thin films with different thicknesses of 40, 65, and 90 nm were then deposited. In this

study, bis(10-hydroxybenzo[*h*]quinolino)beryllium (Bebq<sub>2</sub>) of 30 nm with high electron mobility, is used as an electron transport layer (ETL) material to show more balanced carrier transport characteristics.<sup>10</sup> Device structures of phosphorescent OLEDs are also shown in Table I. 40 nm NPB and 30 nm Bebq<sub>2</sub> was used as HTL and ETL, respectively. The EML with 30 nm consisted of OXD or CBP host materials with different concentrations of Ir(ppy)<sub>3</sub>. 2,9-dimethyl-4,7-diphenyl-1,10-phenanthroline (BCP) was used as a hole blocking layer (HBL) material with the thickness of 10 nm. The concentrations of the Ir(ppy)<sub>3</sub> which varied are 0%, 3%, 5%, 9%, and 15% in the OXD- and 9% in the CBP-based devices, respectively.

Figures 1(a)–1(c) shows the normalized electroluminescence (EL) spectra of devices 1, 2, and 3 at different driving voltages, respectively. Molecule structure of our OXD is also shown in Fig. 1(a). As shown in Fig. 1(a), while the thick-

TABLE I. Layer structures of the OLED devices (unit: nm).

Device	EML						
	HTL NPB	Host OXD	Dopant (%) Ir(ppy) <sub>3</sub>	HBL BCP	ETL Bebq <sub>2</sub>	EIL LiF	Cathode Al
1		40					
2		65	0	0			
3		90					
4			0				
5	40		3		30	1.2	100
6		30	5				
7			9	10			
8			15				
Device	NPB	CBP	Ir(ppy) <sub>3</sub>	BCP	Bebq <sub>2</sub>	LiF	Al
9		30	9				

<sup>a)</sup>Electronic mail: jhlee@cc.ee.ntu.edu.tw

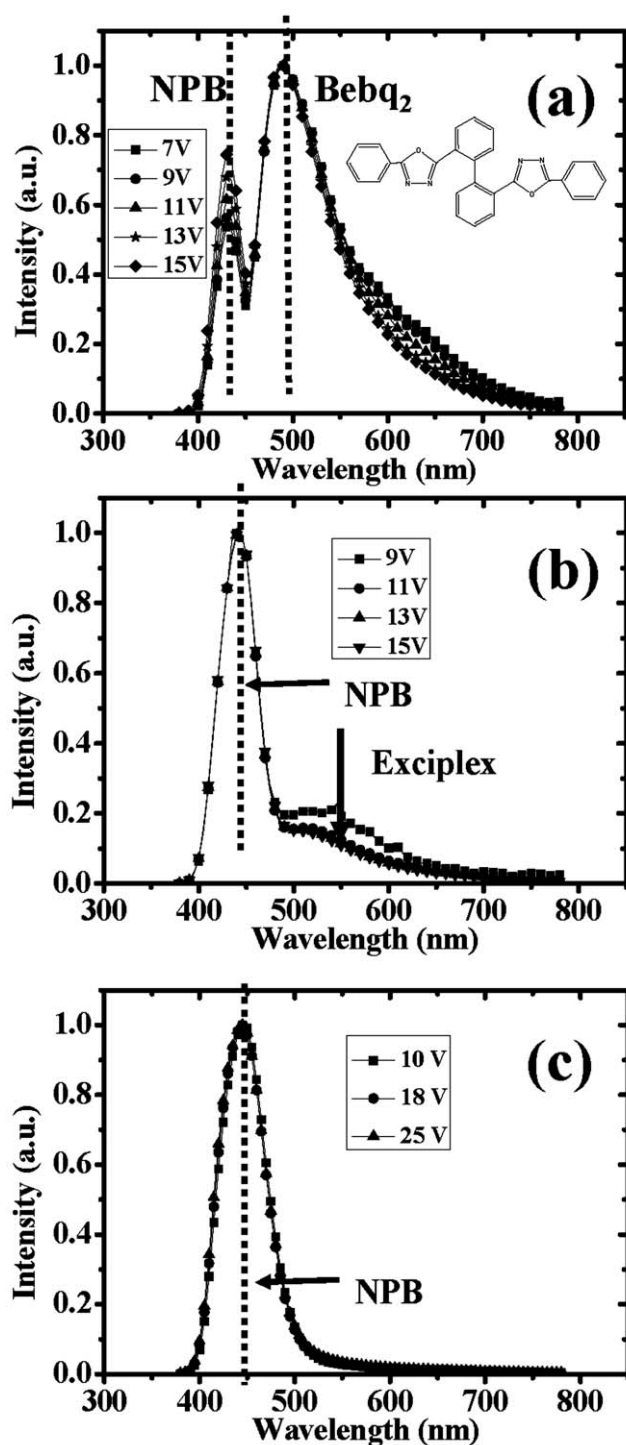


FIG. 1. Electroluminescence spectra of device (a) 1, (b) 2, and (c) 3 with different driving voltages. Molecular structure of our OXD is also shown in Fig. 1(a).

ness of OXD was 40 nm, two peaks at 440 and 490 nm from the NPB and Bebq<sub>2</sub> were observed. That means our OXD materials can both transport the electrons and holes. When increasing the OXD thickness to 65 nm, as shown in Fig. 1(b), we can see that the Bebq<sub>2</sub> peak disappeared and a small hump at 550 nm was observed at a lower driving voltage, 9 V, which may come from the exciplex at Bebq<sub>2</sub> and OXD interface. It shows that the electrons transport through the OXD layer and recombine with holes at NPB layer. On the other hand, the holes are mainly blocked by the OXD that explains the NPB emission. Typically, OXD derivatives are

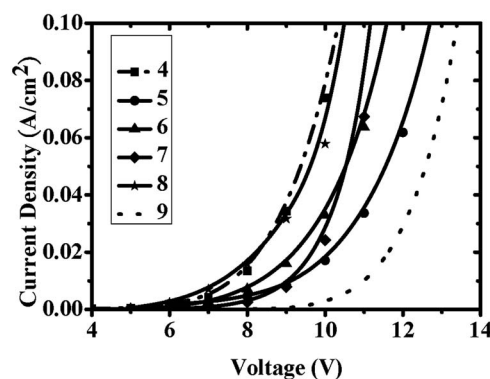


FIG. 2. Comparison of current density vs voltage among devices 4–9.

regarded as an ETL material. However, our OXD exhibits a low HOMO value, i.e., 5.9 eV, which helps hole injection and tunneling through the OXD provided that this layer is thin enough. With increasing the driving voltage, the hump at 550 nm decreases and the electron current dominates under larger electric field. When the OXD further increases to 90 nm [Fig. 1(c)], only NPB peak remains. The holes are totally blocked by the OXD layer.

Figure 2 shows current density and voltage curve ( $J$ - $V$ ) characteristics of devices 4–9. Under the current density of 100 mA/cm<sup>2</sup>, the driving voltage of the OXD- and CBP-based device with 9% dopant concentration are 13.5 and 11.1 V, respectively. Since the HOMO values of NPB, OXD, and CBP are 5.7, 5.9, and 6.3 eV, respectively, the HOMO difference of NPB/OXD is smaller than that of NPB/CBP which results in better hole-injection capability from the HTL into the EML, and hence lower driving voltage in OXD-based devices. With Ir(ppy)<sub>3</sub> concentration in OXD increases from 0% to 15% (devices 4–8), the driving voltage under the current density of 100 mA/cm<sup>2</sup> increases rapidly then decreases from 10.3, 12.7, 11.5, 11.1, to 10.5 V. As described before, our OXD is preferred to transport electrons than holes. On the other hand, Ir(ppy)<sub>3</sub> exhibits the capability to transport holes.<sup>8</sup> Holes (electrons) hop among the Ir(ppy)<sub>3</sub> (OXD) molecules in the EML. When the doping concentration is low, the distance between the Ir(ppy)<sub>3</sub> molecules are large and act like a hole trap which impedes further hole injection and the voltage increases. However, when the doping concentration increases, the hole mobility increases since the distance between the Ir(ppy)<sub>3</sub> molecules decreases, which means that direct recombination of carriers on dopant material (i.e., carrier trapping effect) is possible in our phosphorescent OLED.<sup>11</sup> Such ambipolar transport characteristics of the EML effectively decrease the driving voltage. From the absorption and photoluminescence spectra of Ir(ppy)<sub>3</sub> and OXD (not shown here), good spectrum overlap between the host emission (356 nm) and the absorption of the singlet metal-to-ligand charge-transfer state of Ir(ppy)<sub>3</sub> (389.5 nm) was observed which means an efficient energy transfer from OXD to Ir(ppy)<sub>3</sub>. From EL spectra, we did not observe obvious difference among devices 5–8, which means that the energy transfer from OXD to Ir(ppy)<sub>3</sub> is efficient even the dopant concentration is as low as 3% (device 5).<sup>11</sup>

Figure 3 shows the curves of current efficiency versus current density. With increasing the Ir(ppy)<sub>3</sub> concentrations from 3%, 5%, 9%, to 15%, the current efficiency increases then decreases from 10.4, 13, 24, to 17 cd/A at the lumi-

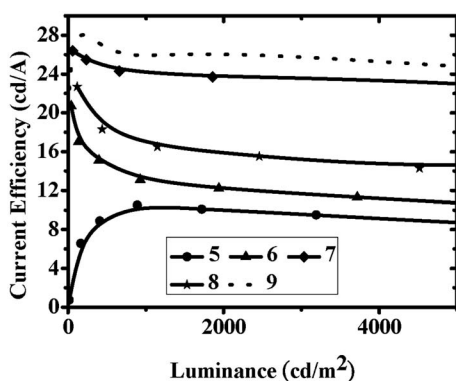


FIG. 3. Comparison of current efficiency vs luminance among devices 5–9.

nance of 1000  $\text{cd/m}^2$ . In a phosphorescent OLED, the current efficiency typically decreases rapidly with increasing driving current due to severe triplet-triplet annihilation.<sup>12</sup> However, in our device 5 [ $\text{Ir}(\text{ppy})_3=3\%$ ], the current efficiency increases rapidly then decreases slowly with increasing the driving current. That means that the carriers are imbalance in such a device, i.e., more electrons than holes in the recombination zone. With increasing the  $\text{Ir}(\text{ppy})_3$  concentrations in the EML, its hole mobility increases and charge balance condition is satisfied. The current efficiency of the conventional CBP-based OLED (device 9) is 25.9  $\text{cd/A}$  at the luminance of 1000  $\text{cd/m}^2$ . Compared to our optimized OXD-based OLED (device 7), the current efficiency of CBP-based device is slightly higher. However, since the driving voltage of the OXD-based device is lower, the power efficiency increases, from 8 to 10  $\text{lm/W}$ , when the host material is changed from CBP to OXD.

To obtain the device stability information, we performed the accelerated operation lifetime of devices 7 and 9 with an initial luminance of 10 000  $\text{cd/m}^2$ . The resulting half-lifetime are 46 and 119 min for the BCP- and OXD-based materials. The low lifetime values are due to the very high initial luminance.<sup>13</sup> We can see that the half-lifetime of the OXD-based device was about 2.6 times longer than that of the CBP-based one which is due to (1) the higher glass tran-

sition temperature (over 200  $^\circ\text{C}$ ) of OXD material and (2) ambipolar carrier transport characteristics which broaden the recombination zone.<sup>14</sup>

In summary, we have shown a phosphorescent OLED based on OXD derivative as the host of the EML which exhibits a lower driving voltage, higher power efficiency, and a longer lifetime compared to the conventional CBP-based OLED. The low driving voltage comes from the low HOMO value and ambipolar transport characteristics. The long lifetime is due to the broaden recombination zone and the high  $T_g$  value of the OXD.

This work was supported by the National Science Council, Republic of China, under Grant Nos. NSC 95-2221-E-002-305 and NSC 95-2113-M-002-020.

<sup>1</sup>C. W. Tang and S. A. VanSlyke, *Appl. Phys. Lett.* **51**, 913 (1987).

<sup>2</sup>C. W. Tang, S. A. VanSlyke, and C. H. Chen, *J. Appl. Phys.* **65**, 3610 (1989).

<sup>3</sup>F. Li, M. Zhang, J. Feng, G. Cheng, Z. Wu, Y. Ma, S. Liu, J. Sheng, and S. T. Lee, *Appl. Phys. Lett.* **83**, 365 (2003).

<sup>4</sup>G. He, M. Pfeiffer, K. Leo, M. Hofmann, J. Birnstock, R. Pudzych, and J. Salbeck, *Appl. Phys. Lett.* **85**, 3911 (2004).

<sup>5</sup>M. Pfeiffer, S. R. Forrest, X. Zhou, and K. Leo, *Org. Electron.* **4**, 21 (2003).

<sup>6</sup>C. Adachi, M. A. Baldo, S. R. Forrest, and M. E. Thompson, *Appl. Phys. Lett.* **77**, 904 (2000).

<sup>7</sup>M. K. Leung, C. C. Yang, J. H. Lee, H. H. Tsai, C. F. Lin, C. Y. Huang, Y. O. Su, and C. F. Chiu, *Org. Lett.* **9**, 235 (2007).

<sup>8</sup>M. A. Baldo, S. Lamansky, P. E. Burrow, M. E. Thompson, and S. R. Forrest, *Appl. Phys. Lett.* **75**, 4 (1999).

<sup>9</sup>J. H. Lee, M. H. Wu, C. C. Chao, H. L. Chen, and M. K. Leung, *Chem. Phys. Lett.* **416**, 234 (2005).

<sup>10</sup>J. H. Lee, C. I. Wu, S. W. Liu, C. A. Huang, and Y. Chang, *Appl. Phys. Lett.* **86**, 103506 (2005).

<sup>11</sup>R. J. Holmes, B. W. D'Andrade, S. R. Forrest, X. Ren, J. Li, and M. E. Thompson, *Appl. Phys. Lett.* **83**, 3818 (2003).

<sup>12</sup>Y. J. Su, H. L. Huang, C. L. Li, C. H. Chien, Y. T. Tao, P. T. Chou, S. Datta, and R. S. Liu, *Adv. Mater. (Weinheim, Ger.)* **15**, 884 (2003).

<sup>13</sup>R. C. Kwong, M. R. Nugent, L. Michalski, T. Ngo, K. Rajan, Y. J. Tung, M. S. Weaver, T. X. Zhou, M. Hack, M. E. Thompson, S. R. Forrest, and J. J. Brown, *Appl. Phys. Lett.* **81**, 162 (2002).

<sup>14</sup>H. Aziz, Z. D. Popovic, N.-X. Hu, A.-M. Hor, and G. Xu, *Science* **283**, 1900 (1999).